Textures and Microstructures, 1996, Vol. 28, pp. 1–15
Reprints available directly from the publisher.
Photocopying permitted by license only

NEUTRON TEXTURE INVESTIGATIONS ON NATURAL MT. ISA CHALCOPYRITE ORE. PART II: PREFERRED ORIENTATION OF CHALCOPYRITE AFTER DIFFERENT EXPERIMENTAL DEFORMATION CONDITIONS

E. M. JANSEN[1], H.-G. BROKMEIER[2] and H. SIEMES[1]

[1]*Institut für Mineralogie und Lagerstättenlehre, RWTH Aachen, Wüllnerstr. 2, D-52056 Aachen, Germany*
[2]*Institut für Metallkunde und Metallphysik, TU Clausthal, Außenstelle GKSS Forschungszentrum, Postfach 1160, D-21494 Geesthacht, Germany*

(Received 10 September 1995)

Natural chalcopyrite samples from Mt. Isa, Australia were axially shortened at a constant confining pressure of 300 (400) MPa, at different temperatures from 25–450°C, in the strain rate range of $3 \cdot 10^{-5}$–$6 \cdot 10^{-8} sec^{-1}$. Neutron diffraction texture analyses of all deformed samples were carried out and compared to the preferred orientation before the experimental deformation.

The preferred orientation of the experimentally undeformed samples consists of three main orientation components, which become weaker with deformation at temperatures to 200°C. One or two new components (A, B) develop with the c-axes perpendicular to the principal strain direction. At a deformation temperature of 250°C and to slower strain rates at 200°C the relics of the original components are stronger. After deformation at temperatures of 300°C to 450°C in general two different types of preferred orientation were detected. One type (2NF) shows two different new components (A*, C), the original components are completely dissolved. The other type (IN) shows the original components partially more concentrated, especially to slower strain rates, and shifting into the directions of the new components of the type 2NF.

KEY WORDS: Chalcopyrite, experimental deformation, temperature, strain rate, neutron diffraction, preferred orientation, pole figure.

INTRODUCTION

The aim of the present study is to elucidate the deformation textures of natural Mt. Isa chalcopyrite after different experimental deformation conditions. This is only possible, if the preferred orientation of the experimentally undeformed material is known. A distinct preferred orientation of the undeformed Mt. Isa chalcopyrite ore was not detectable by X-ray texture analysis, which is shown in a previous extensive study on the deformation behaviour of this ore (Jansen *et al.*, 1993). However, neutron texture analysis is much more sensitive to weak textures than X- ray diffraction (Brokmeier 1994). Thus, a new series of Mt. Isa chalcopyrite analysed by neutron diffraction has revealed a distinct preferred orientation for the experimentally undeformed ore (Part I of this contribution, Jansen *et al.*, 1995). As the deformation induced preferred

orientation is distinguished now from the original preferred orientation, an investigation of all samples of the previous series was carried out by neutron diffraction.

STARTING MATERIAL AND EXPERIMENTAL

The average composition of the Mt. Isa ore is: 85% chalcopyrite, 3% pyrrhotite, 1% pyrite and 11% quartz and other minerals, the average grain diameter of chalcopyrite being 0.3 mm. Collectively 28 cylindrical specimens of 30 mm in length and 15 mm in diameter had been axially shortened in two series (Jansen *et al.*, 1993, 1995). A constant confining pressure of 300 MPa (400 MPa for room temperature), temperatures in the range 25–450°C and strain rates in the range $3 \cdot 10^{-5}$–$6 \cdot 10^{-8} sec^{-1}$ were used for shortening test to 32% total strain. The detailed deformation conditions are given in Table 1. Neutron texture analyses were performed at the TEX-2 equipment, GKSS

Table 1 Experimental deformation conditions

Sample No.	*Temperature (°C)*	*Strain rate (sec^{-1})*	*Total strain (%)*	*Run dur.*	*$\Delta\sigma$ (ε = 10%) (MPa)*
CH8505	25	$2.2 \cdot 10^{-5}$	9.30	1.5h	(848)
CH8311	25	$2.6 \cdot 10^{-5}$	16.14	2.0h	888
CH8307	25	$2.5 \cdot 10^{-5}$	17.26	2.1h	783
CH8218	25	$2.4 \cdot 10^{-5}$	24.82	3.1h	869
CH8318	100	$2.4 \cdot 10^{-5}$	9.54	1.4h	(807)
CH8503	100	$2.6 \cdot 10^{-5}$	11.76	1.5h	775
CH8310	100	$2.6 \cdot 10^{-5}$	17.34	2.1h	748
CH8319	100	$2.6 \cdot 10^{-5}$	26.71	3.1h	737
CH8504	200	$2.7 \cdot 10^{-5}$	12.63	1.5h	663
CH8302	200	$2.7 \cdot 10^{-5}$	18.28	2.1h	524
CH8219	200	$2.8 \cdot 10^{-5}$	20.45	2.2h	488
CH8409	200	$2.7 \cdot 10^{-5}$	28.38	3.2h	560
CH8301	200	$6.4 \cdot 10^{-6}$	13.81	6.2h	460
CH8507	200	$2.8 \cdot 10^{-6}$	13.73	15.5h	424
CH8404	200	$2.8 \cdot 10^{-7}$	13.70	6.1d	323
CH8509	250	$2.6 \cdot 10^{-5}$	13.98	1.7h	414
CH8506	300	$2.8 \cdot 10^{-5}$	14.39	1.5h	357
CH8320	300	$2.7 \cdot 10^{-5}$	19.56	2.1h	335
CH8510	300	$2.8 \cdot 10^{-5}$	30.22	3.1h	318
CH8508	300	$2.9 \cdot 10^{-6}$	14.98	15.0h	256
CH8402	300	$2.9 \cdot 10^{-7}$	15.41	6.2d	173
CH8411	400	$2.8 \cdot 10^{-5}$	15.75	1.6h	157
CH8410	400	$2.8 \cdot 10^{-5}$	31.59	3.1h	193
CH8308	400	$2.9 \cdot 10^{-6}$	15.43	15.4h	124
CH8303	400	$3.0 \cdot 10^{-7}$	15.62	6.1h	164
CH8408	400	$6.0 \cdot 10^{-8}$	15.10	29.2d	87
CH8309	450	$2.8 \cdot 10^{-5}$	15.88	1.6h	145
CH8304	450	$2.9 \cdot 10^{-5}$	21.56	2.2h	140

Research Center (Brokmeier, 1989). The (101) and (112) pole figures of chalcopyrite were measured and used to calculate an orientation distribution function (ODF). On one hand the (101) and (112) pole figures were recalculated and on the other hand the non-measured (200), (004), (220) and (204) pole figures were calculated from the ODF (Dahms, 1992). Details of the chalcopyrite neutron texture measuring technique are given in Part I, Jansen *et al.* (1995).

PREFERRED ORIENTATION BEFORE EXPERIMENTAL DEFORMATION

The pole figures of eight undeformed specimens, which showed similar positions and only slight differences of the intensities for the maxima (Jansen *et al.*, 1995), were summed up and mean pole figures were calculated, which are representative for the complete handspecimen from Mt. Isa (Figure 1). The preferred orientation of the starting material consists of three main orientation components, which are single crystal orientations each widely spread around a maximum position. The maxima positions are marked with the symbols 1, 2 and 3 in the (004) mean pole figure (Figure 1), as well as in the (004) pole figures of the deformed samples (Figures 2–8) to point out the preferred orientation changes with deformation. The angles between the compression axis and the maxima positions of the three orientation components are 62, 50 and 55 degrees. The orientation factors of all known chalcopyrite deformation modes for the three orientations are very similar assuming that there is no ideal single crystal orientation but a wide distribution of the crystallites around the maximum positions (Table 2).

Table 2 Schmid factors of the main glide modes of chalcopyrite (Hennig-Michaeli and Couderc, 1989) for the three orientation components of the experimentally undeformed Mt. Isa ore, assuming a distribution of 30 degrees around each maximum position

glide modes (in order of importance)	*Schmid factors for orientation of component* 1 (62°)	2 (50°)	3 (55°)
200°C			
{112} <3–1–1> slip	0.28–0.35	0.26–0.28	0.21–0.24
{112} <–3 1 1> slip	0.30–0.42	0.35–0.45	0.31–0.41
{112} <1 1 –1> twinning	0.25–0.39	0.22–0.24	0.28–0.32
{112} <1 –1 0> slip	0.29–0.49	0.29–0.41	0.27–0.41
{100} <0 1 0> slip	0.13–0.38	0.26–0.30	0.29–0.33
400°C			
{001} <1 1 0> slip	0.34–0.41	0.47–0.49	0.45–0.47
{112} <–1–1 1> slip	0.06–0.12	0.20–0.22	0.15–0.17
{110} <–1–1 1> slip	0.21–0.41	0.31–0.48	0.27–0.47

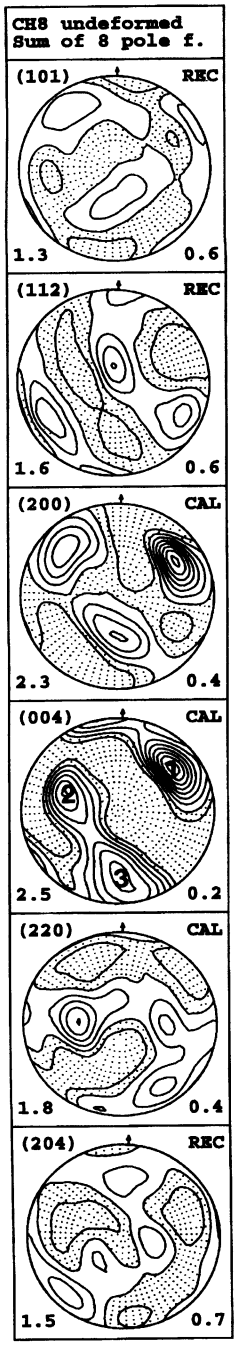

Figure 1 (101), (112), (200), (004), (220) and (204) sum pole figures, each calculated from the pole figures of eight undeformed samples; equal area projection, dotted areas: intensities below 1, contour interval: 0.2, bottom left: maximum, bottom right: minimum intensity.

PREFERRED ORIENTATION AFTER DEFORMATION AT 25 AND 100°C

Figures 2 and 3 each show pole figures of four samples deformed at the same conditions at temperatures of 25 and 100°C varying the total strains. As it is most evident in the (004) pole figures relics of the original three components are still present. They are partially dissolved and shifted. Parts of the components 2 and 3 shifted slightly into the direction of compression axis, and form new central maxima of (101) and (204). Other parts of the original components 1 and 3 shifted to form the new orientation components B and A with the c-axes perpendicular to the principal strain direction. These orientations belong to new central (220) maxima. The strongest component B is developed after 17% shortening at 25°C (CH8307, Figure 2), the strongest component A after 27% shortening at 100°C (CH8319, Figure 3). The sample CH8505 only 9% shortened (Figure 2) does not show a well developed new component in the (004) pole figure, but a central (220) maximum is evident. The dissolution and shifting is different from sample to sample, and no real tendency with increasing total strain is remarkable. The preferred orientation development seems to depend strongly on the exact position and intensity of the original orientation components.

PREFERRED ORIENTATION AFTER DEFORMATION AT 200°C (250°C)

Figure 4 presents the pole figures of four samples deformed at 200°C, a strain rate of $3 \cdot 10^{-5} sec^{-1}$, but different total strains. The original components are more dissolved and the central (204) maxima are of lower intensities than at lower temperatures. Moreover, there is no more central (101) maximum. The development of the new component A seems to be favoured over B. The aspired textural state is a (220) fiber texture. Figure 5 gives the pole figures of four samples deformed with identical total strains, the first three at 200°C decreasing the strain rate from $7 \cdot 10^{-6}$ to $3 \cdot 10^{-7} sec^{-1}$, the fourth at 250°C with the fast strain rate of $3 \cdot 10^{-5}$ sec^{-1}. To slower strain rates at 200°C there is a tendency of the original component 2 to enlarge. The (004) pole figure of sample CH8404, shortened with the slowest strain rate, indicates parts of component 1 shifting into the direction of compression axis. The relics of the original component 1 are of stronger intensity than the new developed component B. A decreasing dissolution of the original components happens at 250°C, parts of component 3 seem to shift towards the position of component 2. Also a tendency of a central minimum in the (101) pole figures is visible, which becomes evident after deformation at higher temperatures (Figures 6, 7, 8).

PREFERRED ORIENTATION AFTER DEFORMATION AT 300°C, 400°C AND 450°C

There are two different kinds of preferred orientation at higher temperatures, explained with Figure 6 which presents the pole figures of four samples deformed at 300°C. Three samples were shortened by 14, 20 and 30% with the same strain rate of $3 \cdot 10^{-5}$ sec^{-1}, and one sample 15% with a 10 times slower strain rate. The first kind of preferred orientation is shown by samples CH8506 and CH8508 after 14 and 15% shortening. The (004) pole figures clearly reveal relics of the original three components. The original

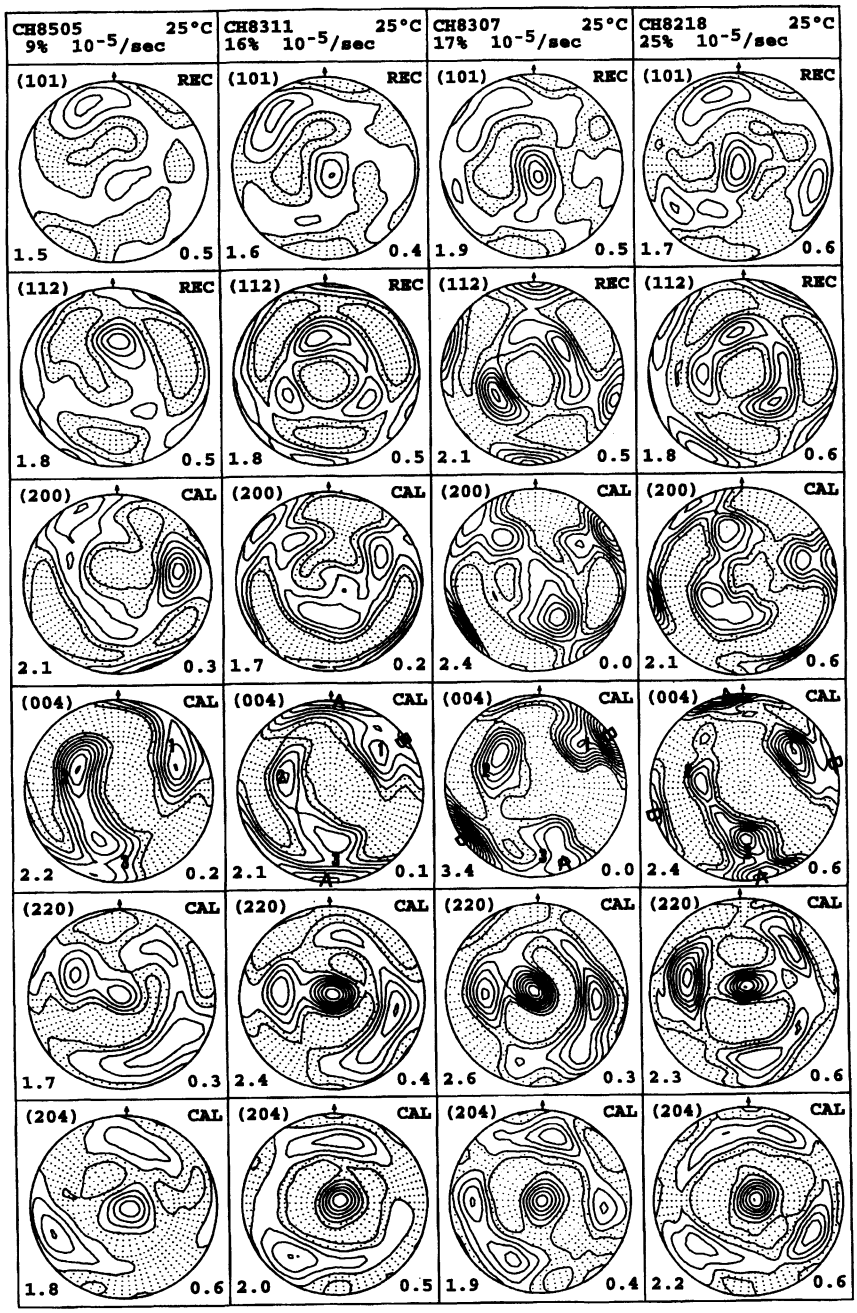

Figure 2 ODF recalculated complete (101) and (112), and calculated (200), (004), (220) and (204) pole figures of samples CH8505, CH8311, CH8307 and CH8218 after experimental deformation at 25°C; equal area projection, dotted areas: intensities below 1, contour interval: 0.2, bottom left: maximum, bottom right: minimum intensity.

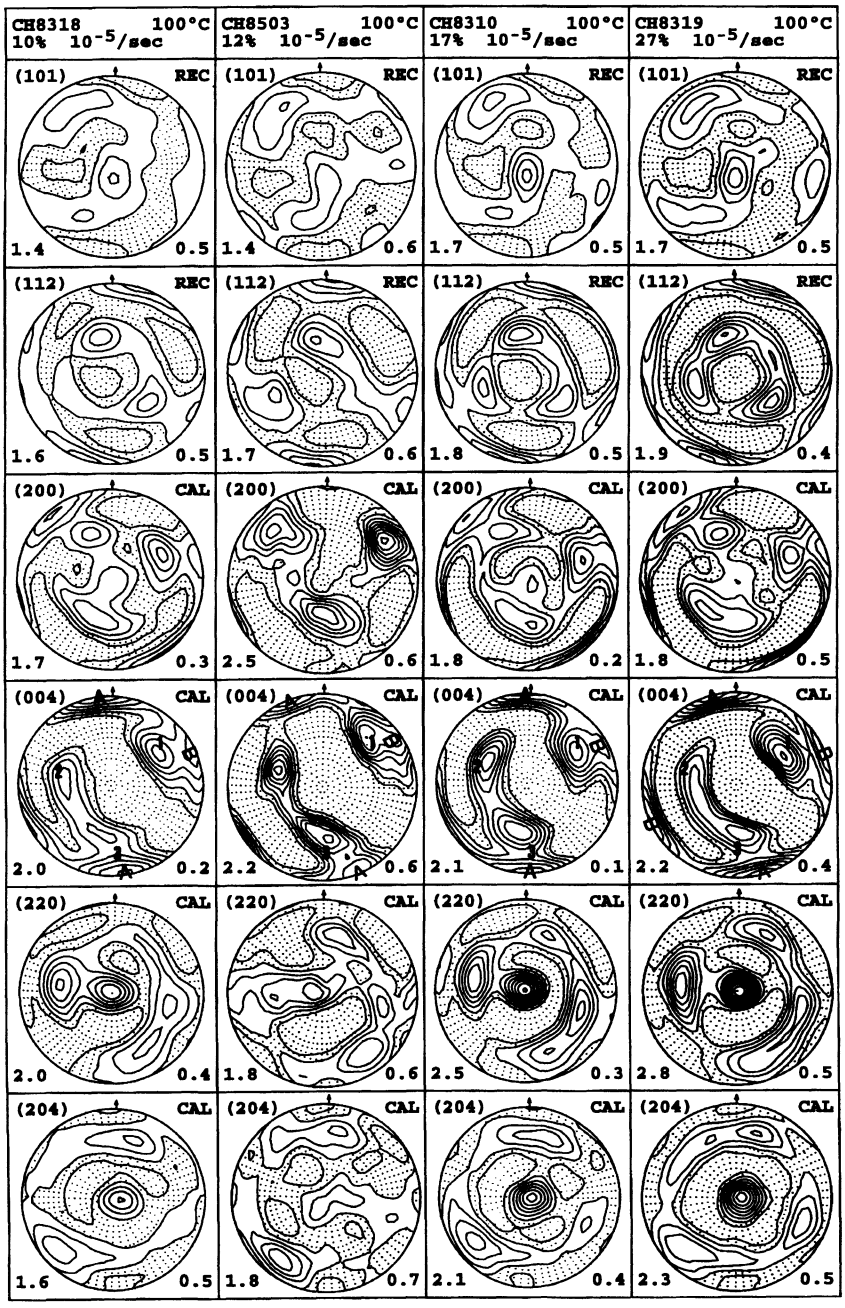

Figure 3 ODF recalculated complete (101) and (112), and calculated (200), (004), (220) and (204) pole figures of samples CH8318, CH8503, CH8310 and CH8319 after experimental deformation at 100°C; equal area projection, dotted areas: intensities below 1, contour interval: 0.2, bottom left: maximum, bottom right: minimum intensity.

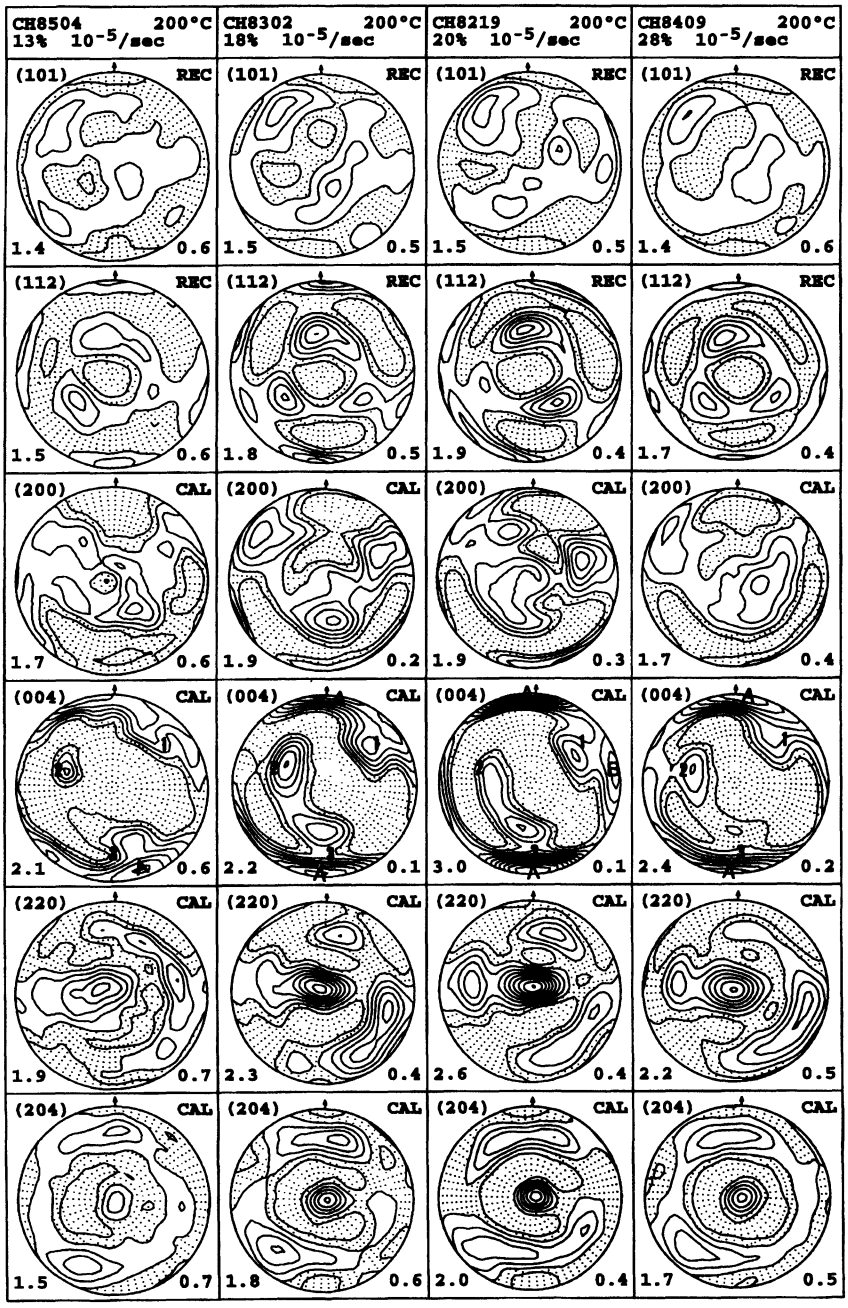

Figure 4 ODF recalculated complete (101) and (112), and calculated (200), (004), (220) and (204) pole figures of samples CH8504, CH8302, CH8219 and CH8409 after experimental deformation at 200°C; equal area projection, dotted areas: intensities below 1, contour interval: 0.2, bottom left: maximum, bottom right: minimum intensity.

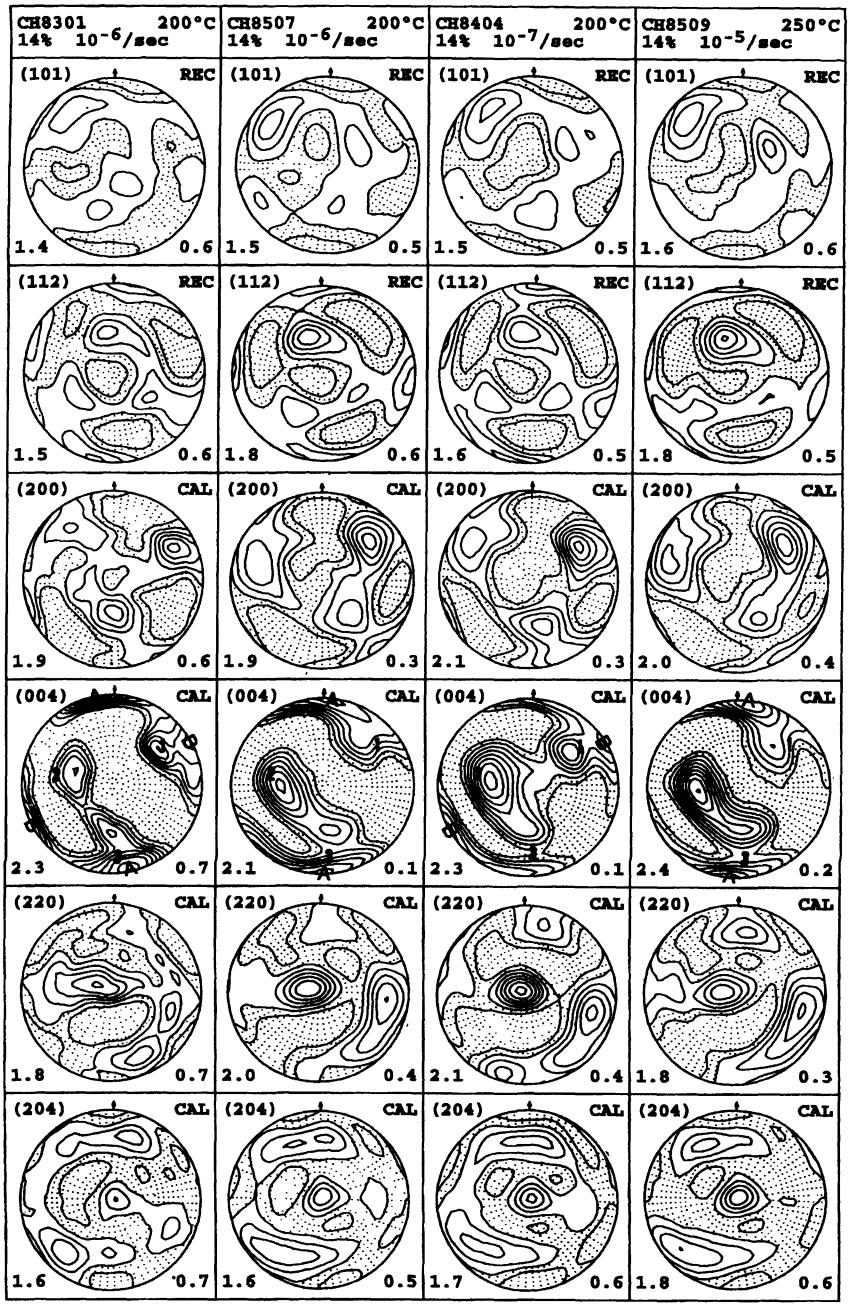

Figure 5 ODF recalculated complete (101) and (112), and calculated (200), (004), (220) and (204) pole figures of samples CH8301, CH8507, CH8404 and CH8509 after experimental deformation at 200°C and 250°C; equal area projection, dotted areas: intensities below 1, contour interval: 0.2, bottom left: maximum, bottom right: minimum intensity.

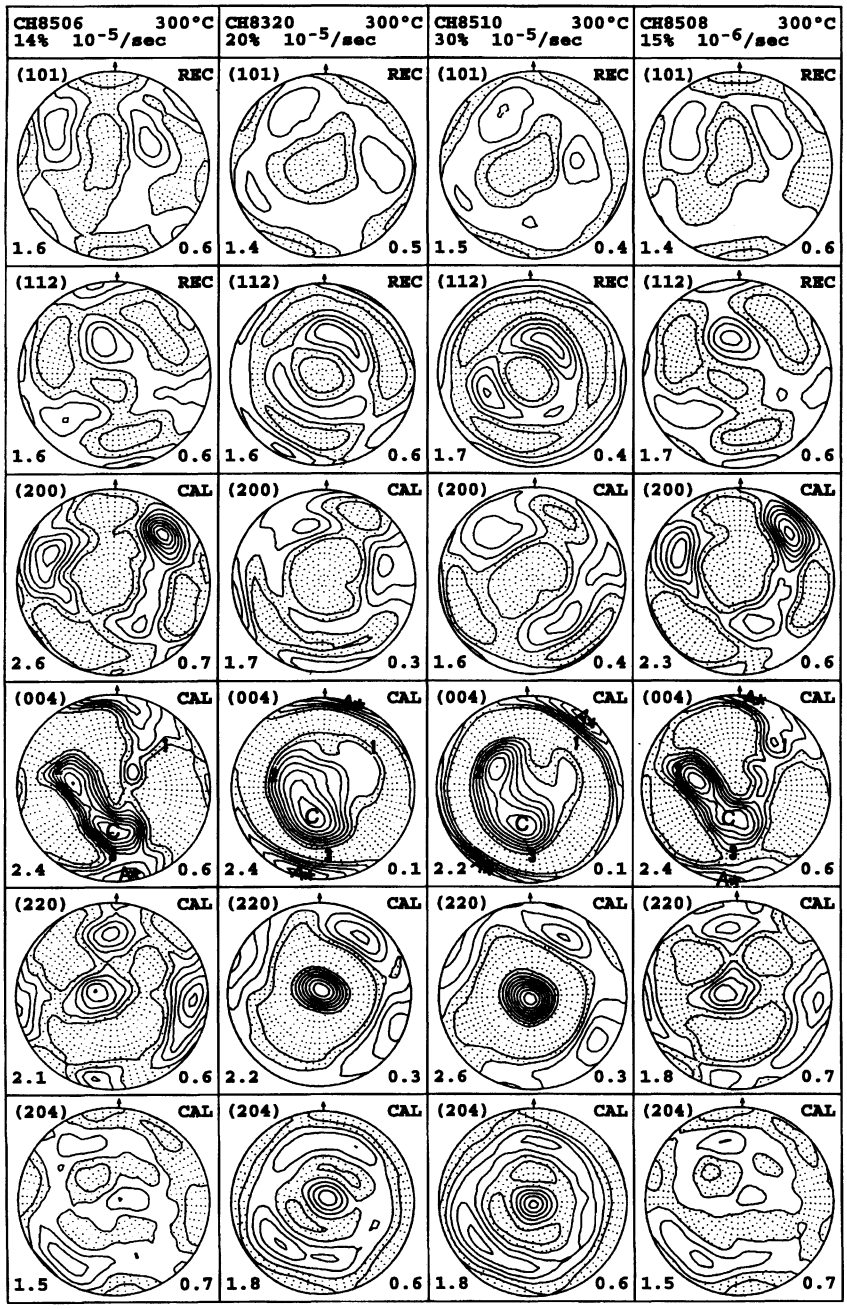

Figure 6 ODF recalculated complete (101) and (112), and calculated (200), (004), (220) and (204) pole figures of samples CH8506, CH8320, CH8510 and CH8508 after experimental deformation at 300°C; equal area projection, dotted areas: intensities below 1, contour interval: 0.2, bottom left: maximum, bottom right: minimum intensity.

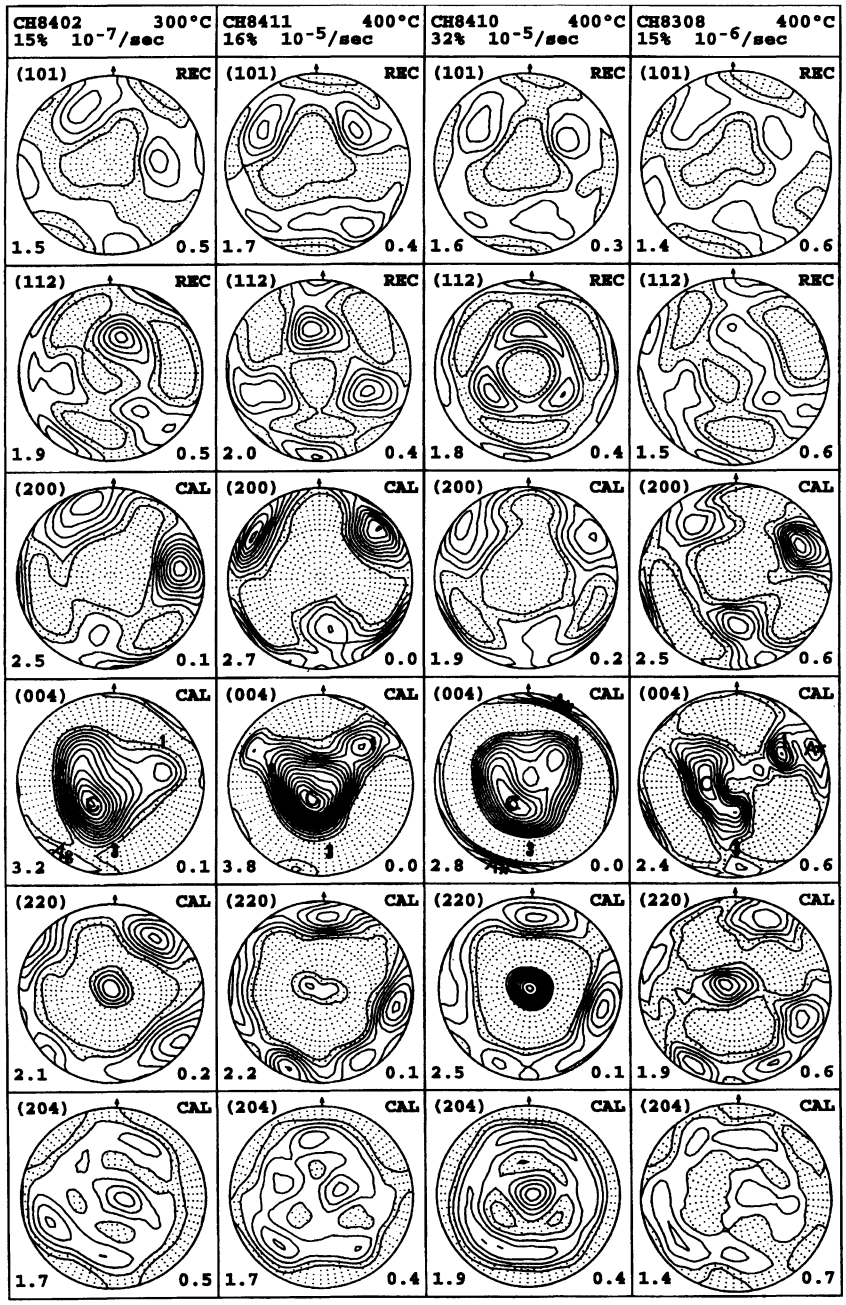

Figure 7 ODF recalculated complete (101) and (112), and calculated (200), (004), (220) and (204) pole figures of samples CH8402, CH8411, CH8410 and CH8308 after experimental deformation at 300°C and 400°C; equal area projection, dotted areas: intensities below 1, contour interval: 0.2, bottom left: maximum, bottom right: minimum intensity.

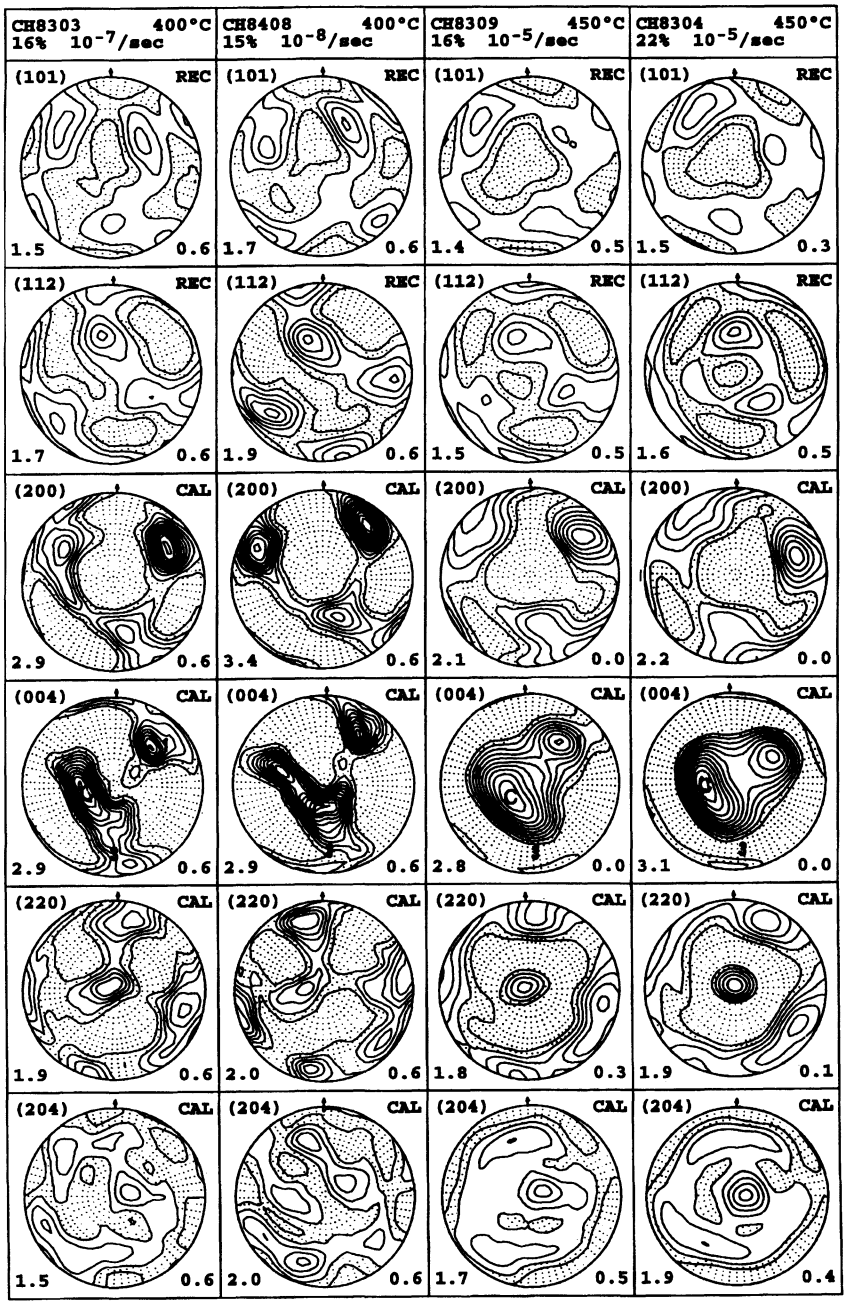

Figure 8 ODF recalculated complete (101) and (112), and calculated (200), (004), (220) and (204) pole figures of samples CH8303, CH8408, CH8309 and CH8304 after experimental deformation at 400°C and 450°C; equal area projection, dotted areas: intensities below 1, contour interval: 0.2, bottom left: maximum, bottom right: minimum intensity.

component 2 and parts of component 3 shifted towards each other and towards the center. Parts of component 1 shifted towards component 3. Parts of 1 and 3 form a not well developed component with the c-axes perpendicular to the principal strain direction. This component is marked with the symbol A*, as there is a clear tendency at higher temperatures to form only one of these components. Central maxima of (220) and (204) are not well developed. As it seems to be an incomplete new texture this type of preferred orientation is called IN. The second kind of preferred orientation is presented by samples CH8320 and CH8510 after 20 and 30% shortening in Figure 6. Each of the samples really shows a new deformation induced preferred orientation, which is nearly a fiber texture consisting of two new fiber components (2NF). The first fiber is produced by component 2 and parts of components 3 and 1, which all shifted towards the center of the pole figures, and tend to form a small circle distribution about 45 degrees off the center, where a maximum C is remarkable. A central (204) maximum belongs to this new orientation component. The second fiber is characterised by a shifting of parts of components 1 and 3 to form a strong developed component A*, according to a strong central (220) maximum. As the shifting of the original components for both kinds of preferred orientations is very similar and a dependence on total strain is obvious, the first kind of preferred orientation (IN) is regarded as intermediate state to the second kind (2NF).

In Figure 7 the pole figures of the slowly at 300°C shortened sample CH8402 show a preferred orientation of the second kind (2NF), but less of components 1 and 3 shifted to form A*. Also sample CH8411, shortened 16% at 400°C with the fast strain rate, shows a preferred orientation similar to the second kind (2NF), but nearly without component A*, and with relics of the original components 1 and 2. The 32% shortened sample CH8410 presents the best developed fiber texture of all investigated samples. Component A* is strong developed and also the small circle distribution in the 2NF-type texture of this sample. Sample CH8308 shortened 15% at 400°C with a ten times slower strain rate presents the IN-type of preferred orientation, with the difference that component 1 shifted towards component 2, and components 2 and 3 shifted nearer to the center. In Figure 8, the preferred orientation of the very slowly at 400°C deformed samples CH8303 and CH8408 is of the IN-type, but a stronger concentration of intensities near the original maxima positions is obvious. A component A* is not really existing. The texture of both samples deformed at 450°C, CH8309 and CH8304, is similar to the 2NF-type texture, but again as most samples after deformation at higher temperatures nearly without component A*.

The aspired textural state seems to be a two-component-fiber texture, if the strain is high enough.

SUMMARY AND CONCLUSIONS

In contrast to the X-ray texture investigations on the Mt. Isa chalcopyrite (Jansen *et al.*, 1993), which only showed more or less incomplete (220/204) fiber textures after different deformation conditions, the neutron texture measurements really give details of textural changes with deformation, provided that the original preferred orientation is well defined. This clearly reveals the present study.

From room temperature to 200°C deformation temperature using fast strain rates an increasing activity of the glide modes is confirmed by an increasing dissolution of the original orientation components. A strain dependence of the dissolution is only clearly

revealed for the samples at 200°C. Considering the high strained samples, a (220) fiber texture must be the aspired textural state. The different {112} glide modes (Table 2) should be responsible for this development, which are reported to be active in single crystals at a deformation temperature of 200°C (Hennig-Michaeli and Couderc, 1989). A change of the activated glide modes is intimated at deformation temperatures of 250°C and 200°C at slow strain rates, and clearly happens at 300°C. (001) slip, which is reported to be the main deformation mechanism at 400°C in single crystals (Hennig-Michaeli and Couderc, 1989), becomes evident. The basal slip system produces the new component C, which is in the ideal case a small circle distribution of (001) 45 degrees off the center. This component belongs to a central (204) maximum in the pole figures, so it is a (204) fiber component. The tendency of the (001) planes to align perpendicular to the principal strain direction is stopped at 30 degrees at the latest, as the orientation factors for the basal glide become to small. The importance of {112} slip decreases with temperature as the stresses are to low. Thus, only the high strained samples at higher temperatures show a well developed (220) fiber component.

To slower strain rates after deformation at temperatures of 200°C and 300°C the preferred orientations become in detail similar to that of higher temperatures. At 400°C to slower strain rates diffusion processes seem to be favoured over glide processes as active deformation mechanisms, as it is also proofed by an increasing phase reaction of chalcopyrite and pyrrhotite to the intermediate solid solution with decreasing the strain rate (Jansen and Siemes, 1993). Only a slight shifting of the original orientation components and a concentration of intensities around their positions happens at these conditions.

As this study has shown, for a deformation induced preferred orientation development under laboratory conditions, the most important factors are not temperature, strain rate or activated glide modes, but the original preferred orientation.

Acknowledgements

The authors wish to thank W. Murach for technical assistance at the TEX-2. B. Eisenlohr gratefully supplied the chalcopyrite ore from Mt. Isa, Australia. EMJ was funded by the Deutsche Forschungsgemeinschaft (Bonn) and HGB by the Bundesministerium für Forschung und Technologie (03BU3CLA F.4-K19).

References

Brokmeier, H.-G. (1989). Neutron Diffraction Texture Analysis of Multi-Phase Systems. *Textures and Microstructures,* **10**, 325–346.

Brokmeier, H.-G. (1994). Application of neutron diffraction to measure preferred orientations of geological materials in: *Textures of Geological materials,* eds. H. J. Bunge, W. Skrotzki, S. Siegesmund, K. Weber, DGM Oberursel, 327–344.

Dahms, M. (1992). The Iterative Series Expansion Method for Quantitative Texture Analysis - Part II: Applications, *J. Appl. Cryst.,* **25**, 258–267.

Hennig-Michaeli, C. and Couderc, J. J. (1989). TEM study of dislocation reactions in experimentally deformed chalcopyrite single crystals in: *Deformation processes in minerals, ceramics and rocks,* eds. Barber, D. J. and Meredith, P. G., Unwin Hyman, London, 391–414.

Jansen, E. M. and Siemes, H. (1993). Phase reaction between chalcopyrite and pyrrhotite during axial compression experiments at 400°C and 450°C, 300 MPa confining pressure and different strain rates. *N. Jb. Miner. Mh.,* **7**, 325–336.

Jansen, E. M. and Siemes, H., Merz, P., H., Schäfer, W., Will, G. and Dahms, M. (1993). Preferred orientation of experimentally deformed Mt Isa chalcopyrite ore. *Miner. Mag.,* **57**, 45–53.

Jansen, E. M., Brokmeier, H.-G. and Siemes, H. (1995). Neutron texture investigations on natural Mt. Isa chalcopyrite ore. Part I: Preferred orientation of one and the same chalcopyrite sample before and after experimental deformation. *Textures and Microstructures*, previous volume.

Kelly, W. C. and Clark, B. R. (1975). Sulfide deformation studies III. Experimental deformation of chalcopyrite to 2000 bars and 500°C. *Econ. Geol.*, **70**, 431–453.

Roscoe, W. E. (1975). Experimental deformation of natural chalcopyrite at temperatures up to 300°C over the strain rate range 10^{-2} to 10^{-6} sec^{-1}. *Econ. Geol.*, **70**, 454–472.